Calculation of two-dimensional infrared spectra of ultrafast chemical exchange with numerical Langevin simulations

Jansen, Thomas la Cour; Knoester, Jasper

Published in:
Journal of Chemical Physics

DOI:
10.1063/1.2806179

Calculation of two-dimensional infrared spectra of ultrafast chemical exchange with numerical Langevin simulations

Thomas la Cour Jansen[a] and Jasper Knoester
Center for Theoretical Physics, University of Groningen, Nijenborgh 4, 9747 AG Groningen, The Netherlands and Zernike Institute for Advanced Materials, University of Groningen, Nijenborgh 4, 9747 AG Groningen, The Netherlands

(Received 18 September 2007; accepted 15 October 2007; published online 18 December 2007)

We combine numerical Langevin simulations with numerical integration of the Schrödinger equation to calculate two-dimensional infrared spectra of ultrafast chemical exchange. This provides a tool to model and interpret such spectra of molecules undergoing chemical processes, such as isomerization and solvent exchange reactions. Two-dimensional infrared spectroscopy has already been used to extract reaction rates for ultrafast chemical reactions. We demonstrate that these spectra are not only sensitive to the rates, but also to the finite duration of the exchange. This is emphasised by comparing with the popular Kubo two-state jump models, which do not account for finite exchange times. © *2007 American Institute of Physics*. [DOI: 10.1063/1.2806179]

I. INTRODUCTION

We talk of chemical exchange when a system is in an equilibrium between two or more chemically different states. This phenomenon has been studied extensively using nuclear magnetic resonance (NMR) spectroscopy.[1–3] Two-dimensional nuclear magnetic resonance (2DNMR) spectroscopy allows the determination of both the chemical equilibrium constants and reaction rates for the involved chemical processes.[2] Processes ranging from organic and inorganic isomerization reactions to phosphorylations in biochemical systems have been subject to such investigations.[3] NMR utilizes radio frequency electromagnetic fields, which limits the time resolution to the regime of reactions slower than a microsecond. For faster chemical reactions the NMR signal, due to motional narrowing, will be a sharp peak at the average chemical shift of the involved chemical species, and hence will not give any information on the reaction rate.

Two-dimensional infrared (2DIR) spectroscopy is a powerful—albeit relatively new and unexplored—experimental technique allowing the measurement of dynamical processes taking place on the femtosecond time scale.[4–7] 2DIR allows the observation of ultrafast chemical exchange taking place on the femto- and picosecond time scales, where NMR experiments fail to distinguish between different chemical species. In the typical 2DIR experiment three infrared pulses are sent through the sample with short time delays between them.[4,5,8] The first pulse brings the system into a coherent superposition of the ground state and a singly excited vibrational state, i.e., a state with one vibrational quantum. During the first time delay, t_1, the vibrations evolve in this coherent superposition. Fourier transforming with respect to t_1 gives the first frequency axis ω_1. The second pulse either brings the system back into the ground state, creates a singly excited state population, or creates a coherent superposition of two singly excited states. During the second time delay, t_2, the vibrations are evolving in either of these states. This time delay is called the mixing time. After the mixing time the system is brought into another coherent superposition. This is either a coherent superposition between the ground state and a singly excited state or between a singly and a doubly excited state. This coherent superposition emits the detected signal that is frequency resolved. The detected frequency gives the second frequency axis ω_3. The emission is not instantaneous and the frequency ω_3 can be obtained by Fourier transforming the total emitted field as a function of the time t_3 elapsed after the mixing time. Much like the familiar infrared absorption spectra the interpretation of spectra obtained with 2DIR is complicated by broad overlapping spectral features. However, it has a much higher time resolution than two-dimensional NMR. The use of infrared pulse lasers allows for a time resolution in the order of 100 fs. 2DIR has already been used to reveal several chemical exchange processes experimentally.[7,9–13] The observed processes typically involve solvent rearrangement or conformational changes.

In this paper we will demonstrate that 2DIR spectra may reveal signatures of the chemical reaction dynamics that go beyond the exchange rates. In particular, we will show that the spectra are sensitive to the finite crossing times between different potential wells. In order to do so, we need to go beyond the Kubo two-state jump models that have been used for 2DIR chemical exchange simulations so far.[14–17] The finite crossing times are expected to become particularly important in ultrafast reactions, where the barrier height is small and a wide distribution of configurations between the potential minima are present. Under these conditions, the 2DIR spectra can better be simulated using a Langevin equation approach that accounts for the detailed shape of the potential energy surface.

Theoretically the chemical exchange in 2DIR has been described with the same rate equation framework that is typically used in the analysis of chemical exchange in

[a]Electronic mail: t.l.c.jansen@rug.nl; thomas.lacour@gmail.com

2DNMR.[14–17] In these simulations the chemical exchange is observed in vibrations that are weakly coupled to the reaction coordinates. The observed vibrations are denoted the system and the reaction coordinates the bath. The bath is assumed to exhibit Markovian behavior, corresponding to exponentially decaying frequency correlation functions. Alternatively 2DIR spectra can be simulated using the cumulant expansion approach.[18] While this allows accounting for non-Markovian effects a disadvantage of this approach is that it relies on the Gaussian behavior of the frequency fluctuations. Because in systems with chemical exchange this does not apply, the cumulant expansion approach is useless in the simulation of their 2DIR spectra. Recently, methods have been developed for simulating the 2DIR spectra from trajectories obtained from molecular dynamics simulations.[12,19–21] These methods are based on solving the time-dependent Schrödinger equation numerically and are not restricted to systems with Markovian or Gaussian behavior, but they do require that a trajectory describing the dynamics can be constructed. This can be done either using molecular dynamics, as was done so far,[12,15,19,21–25] or, in a simpler way, by using Langevin simulations of the essential dynamics.[26–29]

The principle of Langevin simulations is that the motion of a few essential degrees of freedom, denoted the explicit bath, is treated using an effective potential, while the interactions between the explicit bath and the remaining bath degrees of freedom are described using a random fluctuating force. The advantage of Langevin simulations is that the essential dynamics in a limited set of coordinates can be studied by assuming random interactions with the degrees of freedom that do not play a central role for the observed phenomena.

The bath coordinates simulated using the Langevin equation affect the vibrations that one examines in the infrared experiments. This could, for example, be through electrostatic interactions.[15,30,31] The motion of the bath coordinates can then be observed indirectly in the infrared spectrum of the affected vibrational mode. For instance, if two distinct bath configurations exist, this can result in a splitting of the infrared peak for one particular vibration in two separate peaks.[9–12]

Below, we will first demonstrate that the numerical simulation of the Langevin equation works for harmonic models, where analytical solutions are known in the limiting overdamped and underdamped cases. We will then demonstrate the applicability of the method to systems with chemical exchange, using a symmetric double well as an example. The simulations in the double-well potential will be compared with simulations of the corresponding two-state jump model.

The remainder of the paper is organized as follows. In Sec. II we will outline the numerical Langevin simulation method and describe the models that we will simulate. We will present the results of the simulations in Sec. III, along with a discussion of the differences between the various models for chemical exchange. Finally, we will draw our conclusions in Sec. IV.

II. METHOD

We separate the overall system consisting of numerous degrees of freedom into three parts. The first part contains the vibrations that are observed in the spectrum. The second part, denoted the explicit bath, contains a few degrees of freedom that are directly coupled to the observed vibrations. The final part contains all remaining degrees of freedom, which we will call the implicit bath.

The observed vibrations are treated quantum mechanically. They are governed by a Hamiltonian that depends on the explicit bath coordinates and their dynamics will be treated using the time-dependent Schrödinger equation, as will be discussed later. The explicit bath is treated classically and its coordinate(s) x evolve according to the Langevin equation[32–34]

$$m\frac{\partial^2 x}{\partial t^2} = -\frac{\partial U(x)}{\partial x} - m\gamma\frac{\partial x}{\partial t} + F^{\mathrm{fluc}}. \tag{1}$$

This equation describes the motion of a system on a potential surface, $U(x)$, with coordinate x associated with a mass m and a friction coefficient γ. The equation can be generalized in a straightforward manner to treat multiple coupled explicit bath coordinates. The explicit bath is perturbed along the coordinate direction by the random fluctuating force F^{fluc}, which originates from the implicit bath. The latter is assumed to be sufficiently described by a Gaussian-Markovian model and is taken to be independent of the explicit bath and the observed vibrations. This fluctuating force is thus Gaussian white noise with the correlation function

$$\langle F^{\mathrm{fluc}}(t)F^{\mathrm{fluc}}(0)\rangle = \delta(t)\gamma mkT. \tag{2}$$

We use the Langevin equation to construct trajectories of the explicit bath on the potential energy surface given an initial position and velocity. The fluctuating forces are obtained using a Gaussian random number generator[35] and the Langevin equation is propagated using the leapfrog Verlet scheme.[33] The explicit bath is assumed to be independent of the observed vibrations.

The observed vibrations are treated by solving the time-dependent Schrödinger equation[19,20,25]

$$\frac{\partial\phi(t)}{\partial t} = -\frac{i}{\hbar}\boldsymbol{H}(x(t))\phi(t), \tag{3}$$

where the vibrational Hamiltonian $\boldsymbol{H}(x(t))$ depends on the explicit bath coordinates $x(t)$. This equation can be solved numerically by dividing the trajectory into small intervals, during which the Hamiltonian can be assumed to be constant.[19] This allows one to determine the time evolution operator

$$U(n\Delta t + t_0, t_0) = \prod_{m=1}^{m=n} \exp\left(-\frac{i}{\hbar}\boldsymbol{H}(x(m\Delta t + t_0))\Delta t\right), \tag{4}$$

which provides the wave function after n intervals of time duration Δt as follows:

$$\phi(n\Delta t + t_0) = \boldsymbol{U}(n\Delta t + t_0, t_0)\phi(t_0). \quad (5)$$

The time evolution operators are used to calculate the linear and two-dimensional infrared spectra.[4,19,20] More specifically, the linear absorption is given by the Fourier transform of the two-point correlation function of the transition dipole $\boldsymbol{\mu}$

$$I(\omega) = \mathrm{Im}\int_0^\infty dt_1 \frac{i}{\hbar}\langle \boldsymbol{\mu}(\tau_2)\boldsymbol{U}(\tau_2,\tau_1)\boldsymbol{\mu}(\tau_1)\rangle \exp(-i\omega t_1). \quad (6)$$

Here τ_2 and τ_1 are the times when the system interacts with the external field and t_1 is the time between these interactions ($t_1 = \tau_2 - \tau_1$). The 2DIR spectra are given by a double Fourier transform of a sum of six four-point correlation functions. The expressions are given in Eqs. (11)–(13) of Ref. 19.

We will consider different one-dimensional models for the explicit bath. For purposes of testing our method, we first study a harmonic potential

$$U(x) = \tfrac{1}{2}kx^2. \quad (7)$$

It is assumed that the frequency of the observed vibration is simply linearly dependent on the explicit bath coordinate, i.e.,

$$\boldsymbol{H}(t) = (\omega_0 + Wx(t))\boldsymbol{b}^\dagger\boldsymbol{b} - \Delta\boldsymbol{b}^\dagger\boldsymbol{b}^\dagger\boldsymbol{b}\boldsymbol{b}, \quad (8)$$

where ω_0 is the average frequency and W is a measure of the coupling between the observed vibrations and the explicit bath. Δ is the vibrational anharmonicity, which is taken to be independent of the bath for simplicity. $\boldsymbol{b}^\dagger$ and $\boldsymbol{b}$ are the usual Bose creation and annihilation operators. This Hamiltonian is the minimal one describing a three level system. It conserves the number of excitations and therefore does not give rise to lifetime relaxation.

In this particular case of one oscillator, with one singly excited state and a fixed transition dipole, Eq. (6) simplifies to

$$I(\omega) = \mathrm{Im}|\mu|^2 \int_0^\infty \exp[i\omega(t)t]dt, \quad (9)$$

where $\omega(t)$ is the frequency for the singly excited state, i.e., $\omega_0 + Wx(t) - \omega$.

Second, in order to study chemical exchange we will consider a symmetric double-well potential

$$U(x) = \begin{cases} \frac{1}{2}k(x-r)^2, & x \geqslant 0 \\ \frac{1}{2}k(x+r)^2, & x \leqslant 0. \end{cases} \quad (10)$$

Here r is half the distance between the two well minima. The barrier hight is $\frac{1}{2}kr^2$. Also in this case, we consider the Hamiltonian in Eq. (8) to describe the observed vibrations. The reaction rate is obtained using the definition that a reaction has taken place, when the bath coordinate has changed from being on the left side of the left minimum to a position on the right side of the right minimum or vice versa.[26] The lifetime of a state was determined as the time between two successive reaction events, with the above definition of a reaction occurrence.

Finally we will consider a double-well system using a two-state jump model. These types of models, first used by Kubo,[36] have been very successful in the description of, for example, chemical exchange in NMR.[37] Within this model, we treat the motion using two independent coordinates. The first coordinate x is accounting for the motion within the wells with the harmonic potential given in Eq. (7). The second coordinate y describes the motion between the wells; y will take the value $-r$ when in the left well and r when in the right well and a stochastic sudden jump model with a constant jump rate between these two values describes the dynamics of y. The motion within the wells is taken to be unaffected by the jump and changing y will not affect x. The jumping rates are fixed such that they reproduce the number of transition events[26] observed in the real double-well potential. For the jump models the reaction is instantaneous and simply defined to take place when the system changes from one state to the other. Likewise, the lifetime is defined as the time between two such events. The vibrational Hamiltonian is

$$\boldsymbol{H}(t) = (\omega_0 + W(x(t) + y(t)))\boldsymbol{b}^\dagger\boldsymbol{b} - \Delta\boldsymbol{b}^\dagger\boldsymbol{b}^\dagger\boldsymbol{b}\boldsymbol{b}. \quad (11)$$

This type of models has already been used to study chemical exchange in 2DIR spectroscopy.[11,14,15,20,38]

We will also calculate the joint probability distribution (JPD) of the bath coordinates at different times, i.e., the probability that the bath coordinate has the value x_1 at one time and the value x_3 at a time t later. This is given by

$$J(x_1, x_3; t) = \langle \delta(x(0) - x_1)\delta(x(t) - x_3)\rangle, \quad (12)$$

where $\langle\cdots\rangle$ denotes the ensemble average and $\delta(x)$ is the Dirac delta function. In the inhomogeneous limit, where the bath coordinate can be assumed to be constant during the time delays t_1 and t_3 (but not necessarily during t_2) and motional narrowing can therefore be neglected, the 2DIR spectrum for a single vibration linearly coupled to the bath coordinate is essentially given by the JPD. The expression that is used for calculating the 2DIR spectrum in this static limit[39] reduces to the JPD, when only one vibration is considered and the overtone is neglected.

III. RESULTS

For the simulations we use $\omega_0 = 1050\ \mathrm{cm}^{-1}$ and $W = 400\ \mathrm{cm}^{-1}\ \mathrm{nm}^{-1}$. For simplicity we chose the transition dipole matrix element of the observed vibration to be of fixed magnitude and direction. The frequency of the overtone that is observed in the two-dimensional infrared experiments is taken to be equal to twice the fundamental frequency minus the anharmonicity, Δ, of 100 cm^{-1}. The transition dipole between the single and double excited states is taken to follow the harmonic rule and be $\sqrt{2}$ times that of the transition dipole between the ground state and the single excited state. The force constant k is set to 1000 kJ mol^{-1} nm^{-2}. The mass, m, is 10 amu and the temperature, T, is 300 K. For the simulations in the double-well potential given in Eq. (10) the well distance is set to 0.1 nm and the remaining parameters were identical to those used for the harmonic potential. This corresponds to a barrier height of 1.25 kJ mol^{-1} or ~150 K. Both potentials used are shown in Fig. 1. We simulate two different situations. One where the friction coefficient γ is

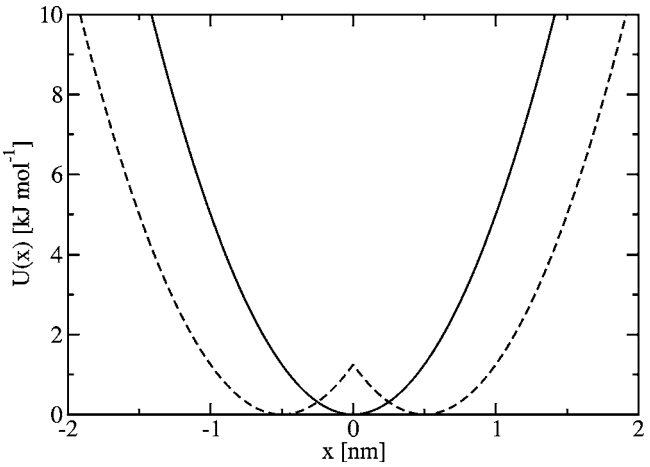

FIG. 1. The potentials used in the simulations. Solid line: harmonic potential used in the overdamped harmonic and underdamped harmonic models. Dashed line: double-well potential used in the overdamped double-well and underdamped double-well models.

50 ps^{-1}, which corresponds to a strong interaction between the explicit and implicit baths. In the other situation γ is 10 ps^{-1} corresponding to a weaker interaction. These two models will be denoted the overdamped and underdamped models, respectively. The Langevin simulations were performed with 10^8 time steps of 1 fs duration. The vibrational Hamiltonian was stored for every ten time steps. The same simulation conditions were used for all models described in this paper.

A. Harmonic models

The autocorrelation functions were obtained for the explicit bath coordinates in the two harmonic models, denoted the overdamped harmonic and underdamped harmonic models, respectively. In the overdamped and underdamped limits analytical expressions are known.[40] In the overdamped limit the correlation function shows a simple exponential decay

$$C(t) = \exp(-\omega_b^2 t/\gamma), \tag{13}$$

where $\omega_b = \sqrt{k/m}$ is the vibrational frequency of the bath coordinate. In our model $\omega_b = 10$ ps^{-1}. The exponential function predicted by the overdamped limit approximation is in good agreement with the correlation function obtained by the numerical simulation for $\gamma = 50$ ps^{-1}. In the underdamped limit the correlation function is given by the damped oscillating function

$$C(t) = \left[\cos(\eta t) + \left(\frac{\gamma}{2\eta}\right)\sin(\eta t)\right]\exp(-\gamma t/2), \tag{14}$$

where $\eta = \sqrt{\omega_b^2 - \gamma^2/4}$ is the frequency of the damped oscillations. In our underdamped model ($\gamma = 10$ ps^{-1}) the value of η is 8.660 ps^{-1}. The function given by the underdamped limit approximation was found to agree very well with the correlation function obtained by numerical simulation.

The linear absorption spectra are shown in Fig. 2 along with Gaussian and Lorentzian fits. For the overdamped harmonic model the Gaussian fit is significantly better than the Lorentzian and vice versa for the underdamped harmonic model. This is what is expected in these two limiting cases.[40]

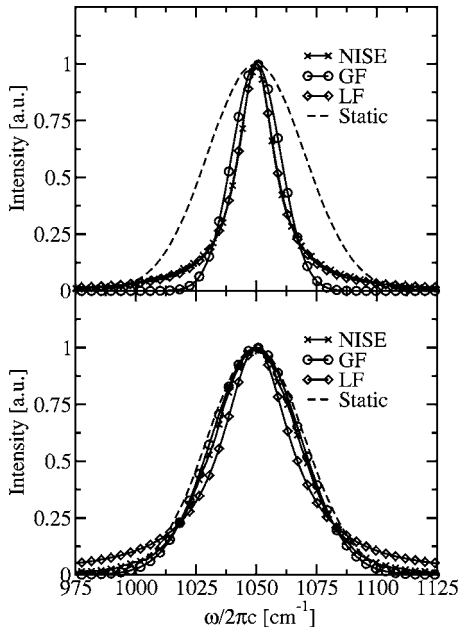

FIG. 2. The linear absorption spectra for the harmonic models. Upper panel: underdamped model. Lower panel: overdamped model. Gaussian and Lorentzian fits are labeled with circles and diamonds, respectively. The dashed black curve indicates the static distribution of frequencies. All graphs were scaled to the same peak height.

From the above results we conclude that our Langevin simulations are capable of recovering all well-known results for simple harmonic models.

B. Double-well and jump models

Again two models for the explicit bath are considered. The parameters for these two models are the same as for the two harmonic models and they are denoted the overdamped double-well and underdamped double-well models. For the jump models the two resulting models are denoted the overdamped jump and underdamped jump models.

For the underdamped double-well model an average of 0.828 transitions are found each picosecond, while 0.314 transitions per picosecond are found for the overdamped double-well model. In Fig. 3 lifetime histograms are shown for the double-well and jump models. At long times the lifetimes of the jump and double-well models are identical. However, for the lifetime distribution the jump models behave exponentially at all times, whereas for the double-well models there is a vanishing probability to find a state with 0 fs lifetime and the distribution peaks at a lifetime of about 500 fs. This is because in the jump model the reaction is instantaneous, while in the double-well model it takes a finite time to travel from the bottom of one well to the bottom of the other.[26]

The linear absorption spectra of the double-well and jump models are shown in Fig. 4. All spectra show a double peak structure corresponding to the well minima. The well minima correspond to frequencies of 1030 and 1070 cm^{-1}. The peak positions for the double-well models are slightly farther away from the center of the band than the well

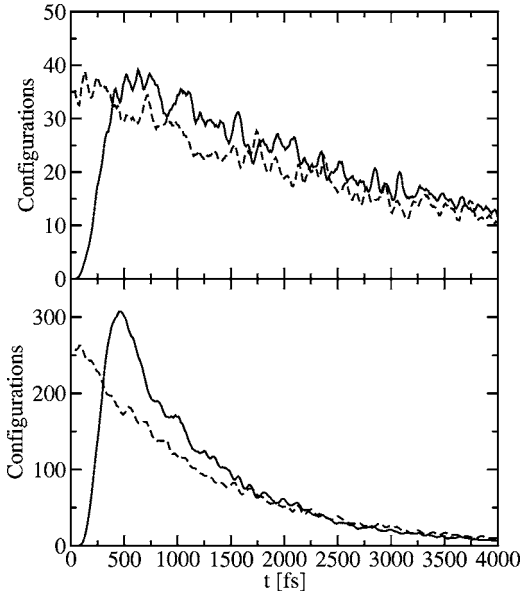

FIG. 3. Lifetime histograms. The number of configurations with a given lifetime is shown using bins with 10 fs width. Upper panel: the overdamped models. Lower panel: the underdamped models. Solid: double-well models. Dashed: jump models.

minima, while the peaks in the jump models are closer to the center. The underdamped models give sharper peaks due to motional narrowing. The difference between the double-well and jump models is striking. The main reason for this is the fact that the two harmonic potentials in the jump model overlap, producing a too high intensity between the peaks.

In Figs. 5–8 the two-dimensional spectra for the different chemical exchange models are shown along with the JPD's of the bath coordinates. These are shown for different waiting times. In the spectra a negative signal is observed in the upper half of the ω_3 interval. This signal originates from ground state bleaching and stimulated emission, while the positive signal in the lower ω_3 arises from excited state absorption. Due to the nature of the models used here, the positive and negative signals are identical, but the excited state absorption is displaced by the 100 cm^{-1} anharmonicity

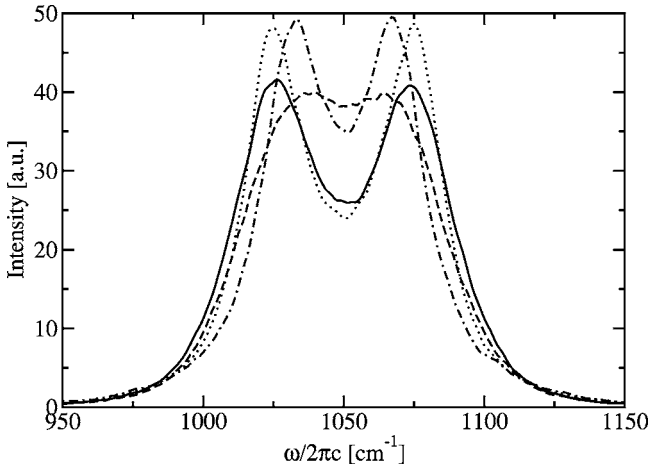

FIG. 4. The linear absorption spectra for the overdamped (full), and underdamped (dotted) double-well as well as the overdamped (dashed) and underdamped (dash-dotted) jump models.

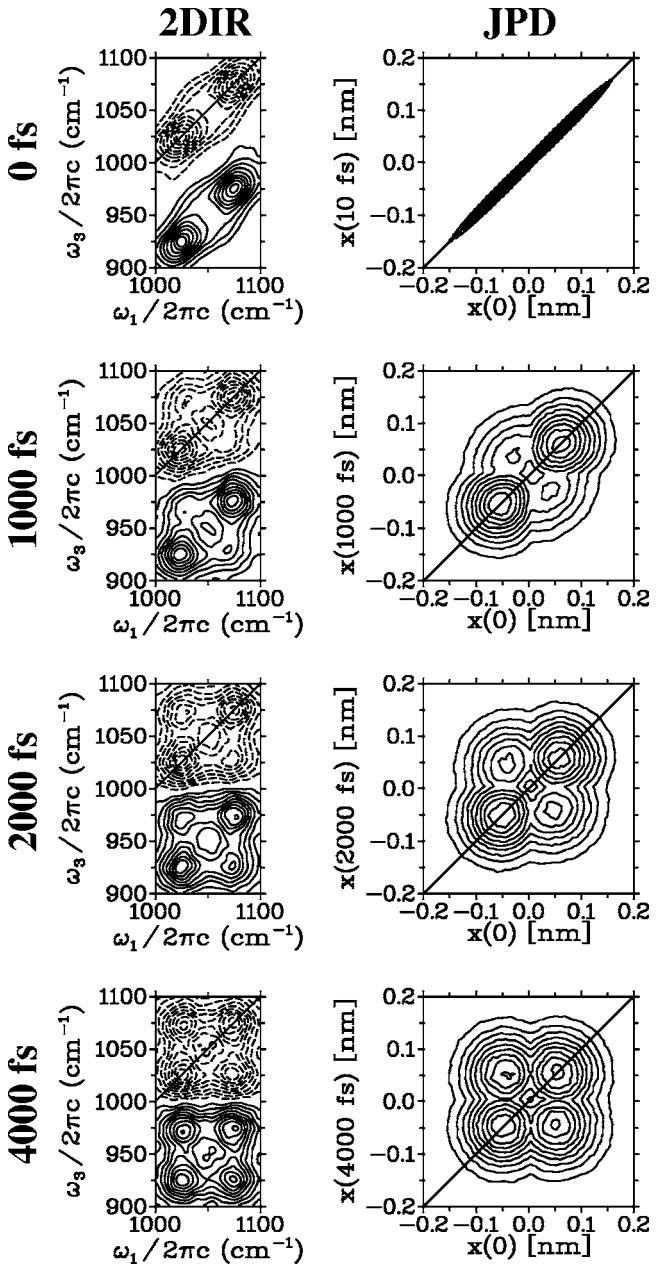

FIG. 5. The 2DIR spectra for the overdamped double-well model with different waiting times and the corresponding joint probability distribution functions of the bath coordinate. In the 2DIR spectra the contour lines for negative absorption, originating from the ground state bleach and stimulated emission contributions, are drawn with dashed lines, while the contour lines for positive absorption, originating from the excited state absorption, are drawn with full lines.

to a lower ω_3 frequency. At zero waiting time no dynamics have taken place and the JPD's are sharply peaked at the diagonal. In the 2DIR spectra some dynamics have occurred during the time intervals where the pump pulses are applied and between the moment when the probe pulse is applied and the signal is measured. Due to the finite duration of the measurement the peaks in the 2DIR spectra are therefore already slightly broadened. This effect is stronger for the underdamped models that exhibit faster dynamics. When the waiting time is increased, cross peaks grow into the spectra, reflecting population transfer between the two configurations. For the overdamped models the 2DIR spectra resemble

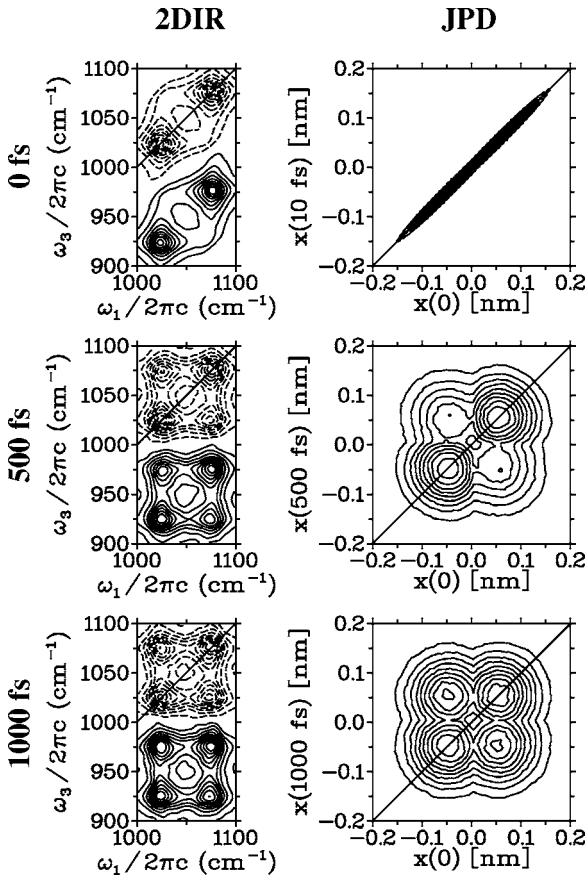

FIG. 6. The 2DIR spectra for the underdamped double-well model with different waiting times and the corresponding joint probability distribution functions of the bath coordinate. The contour lines for the 2DIR spectra are coded as in Fig. 5.

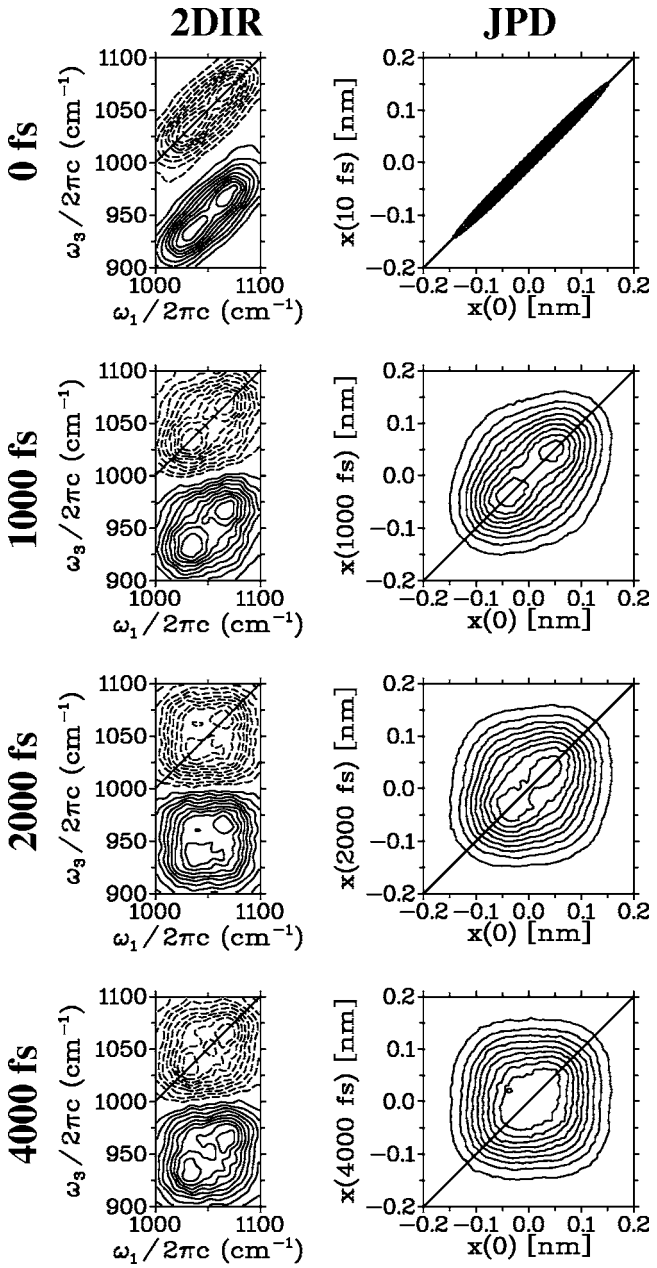

FIG. 7. The 2DIR spectra for the overdamped jump model with different waiting times and the corresponding joint probability distribution functions of the bath coordinate. The contour lines for the 2DIR spectra are coded as in Fig. 5.

the JPD's very well except for at the shortest time. For the underdamped models significant motional narrowing is observed. This leads to the star shaped peaks observed in the 2DIR spectra, in contrast to the round shapes observed in the JPD's.

Differences are observed between the spectra obtained with the double-well and the jump models. As for the linear spectra the most obvious is the larger overlap between the peaks in the jump models. The difference in the time evolution of the two-dimensional spectra is much more subtle and is not directly seen. In order to investigate this, we extracted the population exchange from the spectra. The population exchanged from one well to the other after a given time was found by taking the ratio between the signal integrated over the cross peak area and the sum of the signal integrated over the cross and the diagonal peak areas. The peak intensities were obtained by integrating over a square area centered at the peak. The side length of these squares was 20 cm^{-1}. The results for the overdamped models are shown in Fig. 9. For the jump model an instantaneous increase of the cross peak is observed, reflecting instantaneous population exchange events. On the other hand for the double-well model, it takes a few hundred femtoseconds for the cross peak to start growing, which reflects the finite times needed for the bath coordinate to move from the bottom of one well to the bottom of the other.

The bottom pannel of Fig. 9 displays the time derivatives of the population exchange for both models. As expected the derivative for the jump model exhibits an exponential decay. For the double-well model an initial value close to zero is observed, followed by a peak at about 500 fs. It finally decays with a rate similar to the one observed in the jump model. The zero initial value of the population transfer again clearly reflects the finite time it takes to get from one well to the other. The time scale of this finite crossing time[26] is characterized by the time of 500 fs at which the derivative peaks.

The derivatives can be compared to the lifetime histograms shown in the upper panel of Fig. 3. As expected from the theory of Markovian processes[28,41] for the jump model the exponential decay rate in the lifetime histogram is about

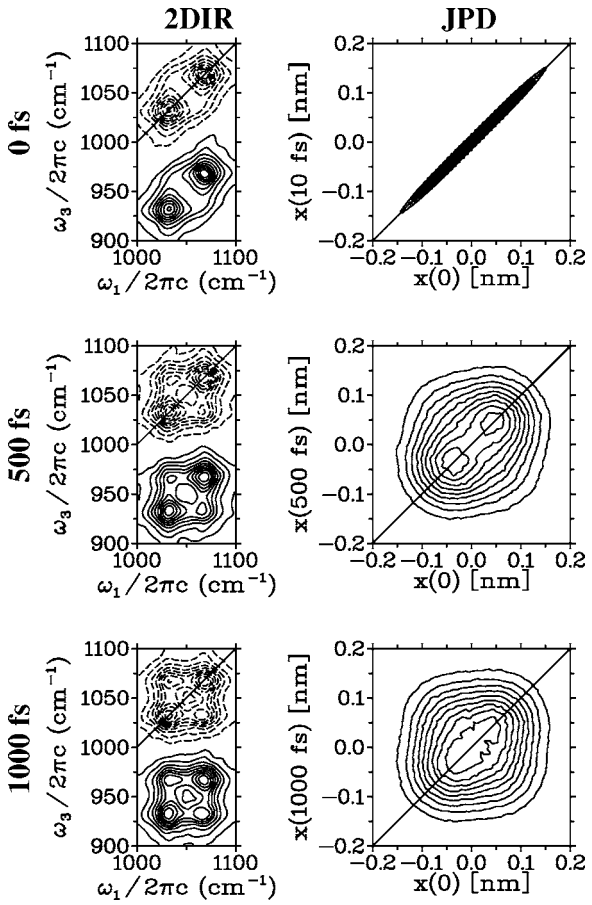

FIG. 8. The 2DIR spectra for the underdamped jump model with different waiting times and the corresponding joint probability distribution functions of the bath coordinate. The contour lines for the 2DIR spectra are coded as in Fig. 5.

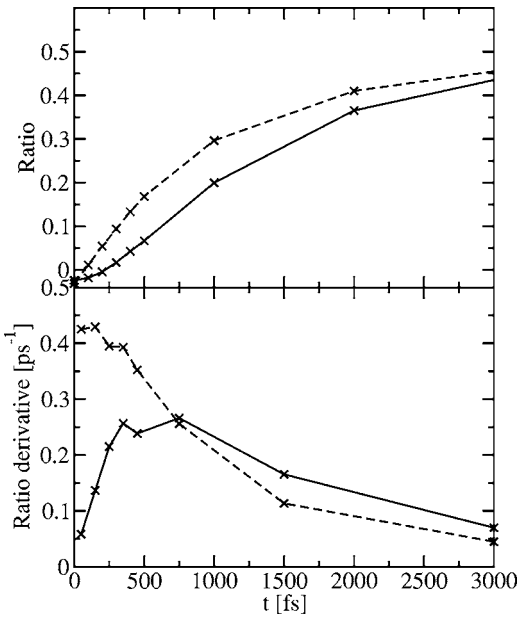

FIG. 9. Upper panel: the 2DIR signal intensity ratio between the cross peak and the sum of the cross and diagonal signals for the overdamped double-well (full line) and overdamped jump (dashed line) models. Lower graph: the time derivative of the ratios in the upper panel.

half the decay rate of the derivative of the population transfer. For the double-well model the derivative of the population transfer and the lifetime distribution both grow from zero at short times and peak around 500 fs, followed by a decay. While the features of the two are similar, there is no direct relation due to the presence of memory in the model. However, the initial time evolution is observed to be very similar and we conclude that the finite time scale of the population transfer can be extracted from the derivative of the population transfer as measured from the two-dimensional spectra.

In the present study a double-well potential with a cusp at the transition state was used. This results in the bath mode being dragged to the bottom of the well as soon as it has passed the transition state and therefore minimizes the finite transfer time. Hence, the used potential provides the toughest conditions for observing the finite transfer time and provides the best test for the possibility of observing this effect. We have also performed simulations with a finite curvature at the transition state, by invoking an adiabatic coupling between the two wells. Tuning the curvature at the transition state such that it is similar to the one at the potential minima, we found little change in the finite transfer time. More importantly, we found that also in this case the 2DIR spectrum reveals information on the finite transfer time. Studying the effect of transition state curvature, temperature, and well distance on the finite transfer time is very interesting,[26] but goes beyond the scope of the present paper.

IV. CONCLUSIONS

In this paper, we analyzed models for chemical exchange processes in which an observed infrared transition is coupled to a bath coordinate moving in a double-well potential. We used a combination of Langevin simulations and numerical integration of the Schrödinger equation (NISE) to calculate the evolution of the observed vibration and its linear and two-dimensional infrared spectra. It was shown that the essential information determining the shape of the spectra is connected to the joint probability distribution of the bath coordinate that modulates the frequency of the observed vibration. The results from the double-well Langevin simulations were compared with two-state jump models, which have previously been used in ultrafast chemical exchange simulations of 2DIR spectra. For the simulated system it was very obvious that the two models that in principle describe the same chemical situation—the movement of a particle between two wells separated by 0.1 nm—give very different results. First, because the Gaussian distributions for the two states in the two-state jump model overlap, resulting in too high a probability for being in the transition region. Second, because in the jump model the transfer between the two states is instantaneous, whereas from the simulations of the actual double-well system the time scale for crossing between both wells was found to be about 500 fs. This finite transfer time is clearly manifested in the 2DIR spectra at short waiting time, simulated for the double-well model, and

we predict that it should be possible to measure it by using this spectroscopy. The interpretation of such experiments should be guided by theoretical simulations.

Numerical Langevin simulations combined with the NISE method is a powerful tool that allows for the calculation of ultrafast chemical exchange. The relatively simple models treated in this paper are just examples demonstrating its potential. The method allows for much more general situations to be investigated. In the present paper we assumed that there was only one infrared active mode in the spectral region of interest. The method can be equally well applied to systems with numerous coupled vibrational modes. Only one explicit bath mode was taken to be important for the spectrum. In practice numerous coupled bath modes can be important; within the present framework these can be treated without problems. A fairly simple potential energy surface was used here, but the method can equally well be applied to more complex surfaces, which, for example, contain more minima or describe angular degrees of freedom as well. A linear relation between the bath coordinate and the frequency of the observed vibration was used, but general functional relationships between the spectral properties and the bath coordinates can be used without complicating the simulations. Finally, the Condon approximation was used, i.e., the transition dipole was assumed to be independent of the bath coordinate. A general functional relationship between these can be used as well.

The combination of Langevin simulations and NISE will allow the simulation and interpretation of 2DIR spectra of chemical exchange of many interesting systems. For example, it might provide more insight into the dynamics of the formation and breaking of hydrogen bonds, a process that is still poorly understood, even in well known liquids such as pure water. It can also be used to study chemical isomerization reactions, the exchange of ligands in inorganic materials, and the exchange of solvent molecules around an infrared active solute. Langevin simulations provide the computational means to answer questions such as how frequently does a chemical reaction occur and how long does it take? 2DIR spectroscopy provides the potential means to experimentally observe the reaction dynamics. The numerical integration of the Schrödinger equation provides the possibility to make a connection between the simulations and the experiments by allowing for calculating the spectra and, thus, for interpreting the experiments.

ACKNOWLEDGMENTS

T.l.C.J. acknowledges the Netherlands Organization for Scientific Research (NWO) for support through a VENI grant.

[1] J. Jeener, B. H. Meier, P. Bachmann, and R. R. Ernst, J. Chem. Phys. **71**, 4546 (1979).
[2] R. R. Ernst, G. Bodenhausen, and A. Wokaun, *Principles of Nuclear Magnetic Resonance in One and Two Dimensions* (Oxford University Press, New York, 1995).
[3] C. L. Perrin and T. J. Dwyer, Chem. Rev. (Washington, D.C.) **90**, 935 (1990).
[4] S. Mukamel, Annu. Rev. Phys. Chem. **51**, 691 (2000).
[5] P. Hamm, M. H. Lim, and R. M. Hochstrasser, J. Phys. Chem. B **102**, 6123 (1998).
[6] Y. Tanimura and S. Mukamel, J. Chem. Phys. **99**, 9496 (1993).
[7] S. Woutersen, Y. Mu, G. Stock, and P. Hamm, Chem. Phys. **266**, 137 (2001).
[8] O. Golonzka, M. Khalil, N. Demirdöven, and A. Tokmakoff, Phys. Rev. Lett. **86**, 2154 (2001).
[9] J. Zheng, K. Kwak, J. B. Asbury, X. Chen, I. R. Piletic, and M. D. Fayer, Science **309**, 1338 (2005).
[10] Y. S. Kim and R. M. Hochstrasser, Proc. Natl. Acad. Sci. U.S.A. **102**, 11185 (2005).
[11] K. Kwak, J. Zheng, H. Chang, and M. D. Fayer, J. Phys. Chem. B **110**, 19998 (2006).
[12] M. F. DeCamp, L. DeFlores, J. M. McCracken, A. Tokmakoff, K. Kwac, and M. Cho, J. Phys. Chem. B **109**, 11016 (2005).
[13] C. Scheurer and T. Steinel, ChemPhysChem **8**, 503 (2007).
[14] F. Sanda and S. Mukamel, J. Chem. Phys. **125**, 014507 (2006).
[15] T. l. C. Jansen, T. Hayashi, W. Zhuang, and S. Mukamel, J. Chem. Phys. **123**, 114504 (2005).
[16] Y. Tanimura, J. Phys. Soc. Jpn. **75**, 082001 (2006).
[17] R. Kubo, in *Fluctuation, Relaxation and Resonance in Magnetic Systems*, edited by D. ter Haar (Oliver & Boyd, Edinburgh, 1962), p. 23.
[18] S. Mukamel, Phys. Rev. A **28**, 3480 (1983).
[19] T. l. C. Jansen and J. Knoester, J. Phys. Chem. B **110**, 22910 (2006).
[20] T. l. C. Jansen, W. Zhuang, and S. Mukamel, J. Chem. Phys. **121**, 10577 (2004).
[21] H. Torii, Chem. Phys. Lett. **414**, 417 (2005).
[22] J. R. Schmidt, S. A. Corcelli, and J. L. Skinner, J. Chem. Phys. **123**, 044513 (2005).
[23] J. R. Schmidt, S. A. Corcelli, and J. L. Skinner, J. Chem. Phys. **121**, 8887 (2004).
[24] T. l. C. Jansen and J. Knoester, J. Chem. Phys. **124**, 044502 (2006).
[25] H. Torii, J. Phys. Chem. A **110**, 4822 (2006).
[26] B. W. Zhang, D. Jasnow, and D. M. Zuckerman, J. Chem. Phys. **126**, 074504 (2007).
[27] M. Berkowitz, J. D. Morgan, and J. A. McCammon, J. Chem. Phys. **78**, 3256 (1983).
[28] R. Zwanzig, *Nonequilibrium Statistical Mechanics* (Oxford University Press, Oxford, 2001).
[29] D. M. Zuckerman and T. B. Woolf, J. Chem. Phys. **116**, 2586 (2002).
[30] T. Hayashi, T. l. C. Jansen, W. Zhuang, and S. Mukamel, J. Phys. Chem. A **109**, 64 (2005).
[31] C. J. Fecko, J. D. Eaves, J. J. Loparo, A. Tokmakoff, and P. L. Geissler, Science **301**, 1698 (2003).
[32] G. D. Billing and K. V. Mikkelsen, *Introduction to Molecular Dynamics and Chemical Kinetics* (Wiley, New York, 1996).
[33] M. P. Allen and D. J. Tildesley, *Computer Simulation of Liquids* (Oxford University Press, Oxford, 1987).
[34] H. A. Kramers, Physica (Amsterdam) **7**, 284 (1940).
[35] G. Marsaglia and A. Zaman, Florida State University Technical report, 1987.
[36] R. Kubo, J. Math. Phys. **4**, 174 (1963).
[37] D. Gamliel and H. Levanon, *Stochastic Processes in Magnetic Resonance* (World Scientific, River Edge, NJ, 1995).
[38] F. Sanda, W. Zhuang, T. l. C. Jansen, T. Hayashi, and S. Mukamel, in *Ultrafast XV*, Springer Series in Chemical Physics Vol. 88 edited by P. Corkum, D. M. Jonas, and R. J. D. Miller (Springer, 2007, 2006), p. 401.
[39] S. Mukamel and D. Abramavicius, Chem. Rev. (Washington, D.C.) **104**, 2073 (2004).
[40] S. Mukamel, *Principles of Nonlinear Optical Spectroscopy* (Oxford University Press, New York, 1995).
[41] H. Risken, *The Fokker-Planck Equation* (Springer-Verlag, Berlin, 1984).